Local Mechanical Properties of Plasma Treated Polystyrene Surfaces

E. Bonaccurso,[†] B. Cappella,*[,‡] and K. Graf[†]

Max Planck Institute for Polymer Research, Ackermannweg 10, D-55128 Mainz, Germany, and Federal Institute for Material Research and Testing, Unter den Eichen 87, D-12205 Berlin, Germany

Received: April 28, 2006; In Final Form: July 20, 2006

We study how a local air plasma treatment affects the mechanical properties of polystyrene by performing indentation measurements on the polymer in the elastic and plastic regime. The local exposure to plasma was obtained by placing a shadow-mask with quadratic holes of 45 × 45 μm^2 on top of the polymer substrate, providing uncovered (exposed to the plasma) and covered (protected from the plasma) areas. We have analyzed quantitatively the topography and the elastic-plastic properties of such a sample with atomic force microscopy (AFM) measurements, both before and after plasma treatment. To enhance the differences between covered and uncovered areas, the sample has been exposed to solvent vapor. This generates regions which are differently swollen. The quantitative investigation of the mechanical properties of the swollen sample for different solvent exposure times gives further insight into the changes of polystyrene mechanical properties caused by the plasma.

Introduction

Surface properties of polymers are extensively studied owing to their great potential in a range of applications. As an example, control of the *wettability* of polymer surfaces is required for patterned growth of cells[1] or to enhance the transport of small liquid samples in microfluidic devices.[2,3] Another example is the requirement to control the *mechanical* properties of polymer materials in processes as hardening, wearing,[4] swelling, and surface structuring.[5] It was found that stretched homopolymers, homogeneously covered with a thin layer of a material with a different elasticity than the bulk, form long-range ordered surface ripples.[6−9] Heterogeneous surfaces, as block copolymers or polymer blends, form 3-D microstructures upon exposure to a solvent, owing to their different response to swelling and shrinking.[10] A confined modification of a homopolymer as polystyrene by a local exposure to plasma through a shadow-mask leads to the formation of permanent protrusions upon heating or exposure to solvent. This has been employed as a microfabrication technique to produce arrays of microwells of different shapes.[11]

The 3-D structures generated by the plasma/solvent treatment can be easily visualized by means of atomic force microscopy (AFM) or optical profilometric microscopy techniques. However, only little is known about the mechanism leading to the formation of the structures, or what the effect of the plasma is. A prerequisite seems to be that the polymer must be extruded or stretched. Additionally, it was found that exposure to a solvent or heating drives the process leading to the rearrangement of the surface topology and to the formation of microstructures. This is a strong hint that a relaxation of oriented polymer chains is most likely the driving force.[12] It has been found that the uncovered areas exposed to plasma form the bottom of the microstructures, whereas the covered areas shadowed by the mask undergo strong swelling and form the top of the microstructures. This observation of a selective swelling suggests that the plasma causes a local chemical transformation, for example cross-linking, of the exposed areas of the polymer. Since cross-linking is known to affect the stiffness of polymers,[13] this suggests that areas locally exposed to plasma should have a different stiffness.

In this paper, we perform quantitative indentation measurements by AFM to *locally* discriminate the mechanical properties of polymers, like their elasticity and plasticity, before and after exposure to plasma and to solvent. The results are discussed and related to the surface topography.

Experimental Section

We used a commercial extruded PS wafer (thickness 1.2 mm, density 1.01 g·cm^{-3}) as a substrate (Goodfellow Ltd, Cambridge, UK), which is protected with a foil against contamination. The molar mass of the extruded PS is broadly distributed (mean number M_n = 109 kg·mol^{-1}, mean weight M_W = 284 kg·mol^{-1}) with a polydispersity index M_W/M_n = 2.6. For the experiments we cut pieces of 15 × 15 mm^2 from the wafer and removed the protection foil. After that, the wafer was cleaned in methanol in an ultrasonic bath for two minutes. All employed solvents have ultrapure grade and were purchased from Fisher Chemicals (Loughborough, UK).

A TEM grid (Plano, Wetzlar, Germany) with quadratic holes of 45 × 45 μm^2 and a ligament width of 20 μm was used as a shadow-mask and placed on the polymer substrate before exposure to the plasma. Afterward, it was exposed for 4 min to air plasma with a power of 60 W and a pressure of 0.1 mbar in a "Femto" plasma generator (Diener Electronic GmbH, Nagold, Germany). In the following, we will refer to the areas of the surface which were shadowed by the mask during the plasma treatment as "covered areas", and to the areas of the surface directly exposed to the plasma as "uncovered areas".

After plasma treatment, the grid was removed, and the polymer substrate was placed in a closed vessel with saturated toluene vapor for 2 min. After removal from the vessel, the substrate was dried for 10 min., and then characterized with

* Corresponding author phone: 49 30 8104-3343; fax: 49 30 8104-2626; e-mail: brunero.cappela@bam.de.
[†] Max Planck Institute for Polymer Research.
[‡] Federal Institute for Material Research and Testing.

10.1021/jp062602w CCC: $33.50
Published on Web 08/18/2006

the AFM (topography and stiffness). This "vapor-drying-measurement" cycle was repeated a second time with the same sample, as explained later. The topography of the sample was acquired after the plasma treatment and after each swelling step with a MFP-3D atomic force microscope (Asylum Research, Santa Barbara, CA) in tapping mode. We used Pointprobe NCL cantilevers (Nanosensors, Wetzlar-Blankenfeld, Germany) with nominal resonance frequency of $f = 160$ kHz and elastic constant $k_c = 40$ N/m, as measured from the noise spectrum of the cantilever. Also, force−distance maps in force−volume mode were recorded with the same cantilever. It is important to remember that the piezo hysteresis is completely corrected in MFP-3D using an inductive displacement control system. The frequency of the force−distance curves (1 Hz) and the scanned area ($80 \times 80\ \mu m^2$) are the same for each measurement. The maximum load $k_c\delta_{max}$ and the total number of force−distance curves were varied. Summarizing, the following force−volume measurements were performed:

(a) 900 curves with $\delta_{max} = 600$ nm after plasma treatment and prior to exposure to toluene vapor;

(b) 900 curves with $\delta_{max} = 100$ nm after 2 min of exposure to toluene vapor;

(c) 2500 curves with $\delta_{max} = 600$ nm after 2 min of exposure to toluene vapor;

(d) as in measurement (c), but only 900 curves, acquired on a different area;

(e) 1600 curves with $\delta_{max} = 600$ nm after 2 additional minutes of exposure to toluene vapor (total exposure time of 4 min.

Results and Discussion

Exposure of polystyrene to a gas plasma, as done in our experiments, leads to etching of the polymer,[5] the etching rate depending primarily on the plasma power, the process time, and the type of gas used. Since in our case, parts of the sample are shadowed by the mask and not exposed to the plasma, we obtain a local plasma etching. This is demonstrated by the height difference of around 20 nm between the uncovered and the covered areas (Figure 1). After exposure to solvent vapor for 2 min., the covered areas of the substrate protrude even more, by about 400 nm. Longer exposure to solvent vapor further increases the height of the protrusions to about 1600 nm. The protrusions on the covered areas persist after the substrate has been removed from the solvent vapor, and even after the swollen substrate has been put into vacuum for several hours in order to remove the solvent more effectively. This is in accordance with earlier results.[9,14]

The height difference between the covered and uncovered areas after the solvent treatment corroborate the hypothesis that the uncovered areas have been superficially cross-linked by the plasma, and that the cross-linked superficial layer hinders polymer chains from protruding. The depth of this superficial layer depends on the plasma treatment parameters. If the treatment time is short and/or the power low, the cross-linking is weak, and the polymer protrudes on both areas after treatment with solvent. In this case only a small height difference between covered and uncovered areas is visible.

The hypothesis formulated on the role of plasma treatment on cross-linking and protruding was investigated in this work by characterizing the elastic and plastic properties of the polystyrene substrate before and after the plasma and solvent treatments.

As a first rough characterization of the mechanical properties, we calculate the stiffness of the sample from the acquired force−distance curves in the limit of small sample deformations. Along

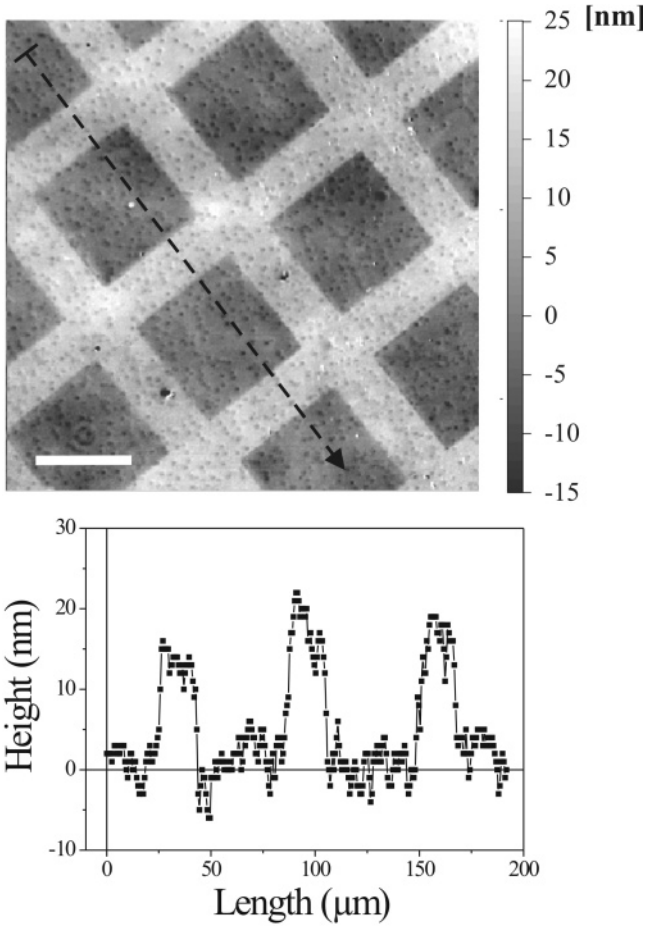

Figure 1. Top: Topography image of a polystyrene substrate exposed to an air plasma (60 W, 4 min) through a shadow mask. White scale bar = 40 μm. Bottom: Profile taken along the black dashed line.

the contact line, i.e., the part of the force−distance curve where tip and sample are in contact, the sample deformation D is given by the following:[15,16]

$$D = Z - \delta \tag{1}$$

where Z is the piezo displacement and δ is the cantilever deflection. If D is small, we can write

$$k_c\delta = \frac{k_c k_s}{k_c + k_s} Z = k_{eff} Z \tag{2}$$

where k_c and k_s are the cantilever and sample elastic constants. This simple relation shows that the slope of the approach force−distance curve is an indicator for the stiffness of the sample. If the sample is much stiffer than the cantilever, i.e., $k_s \gg k_c$, the force−distance curves will probe mainly the stiffness of the cantilever, i.e., $k_{eff} \cong k_c$. If the sample is much more compliant than the cantilever, i.e., $k_s \ll k_c$, the slope of the approach contact line is determined primarily by the stiffness of the sample, i.e., $k_{eff} \cong k_s$. In the following, we calculate the stiffness as the ratio $S = k_{eff}/k_c$ between Z and δ. Therefore, S is dimensionless and $0 < S < 1$.

To examine the mechanical properties of the sample after the plasma treatment and after successive exposures to toluene vapor, we mapped the stiffness from force−distance curves acquired at the border between the covered and uncovered areas. The resulting histograms of all collected data are shown in Figure 2.

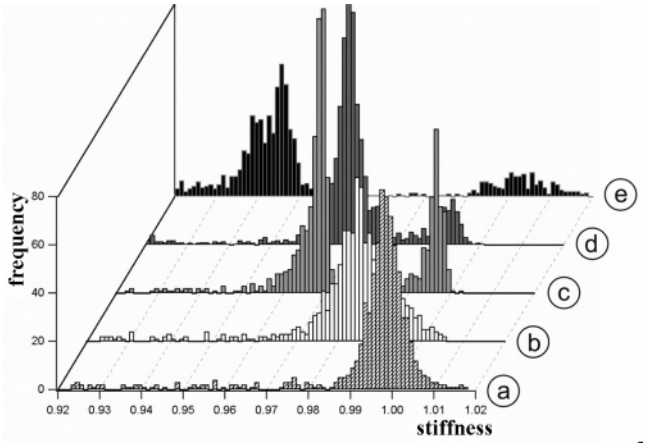

Figure 2. Histograms of the stiffness (as defined in eq 2 and relative text) on polystyrene (PS) after exposure to plasma and to a toluene vapor for x minutes: (a) only plasma through shadow mask; (b) $\delta_{max} = 100$ nm, 900 curves, $x = 2$; (c) $\delta_{max} = 600$ nm, 2500 curves, $x = 2$; (d) $\delta_{max} = 600$ nm, 900 curves, $x = 2$; (e) $\delta_{max} = 600$ nm, 1600 curves, $x = 4$. All histograms are normalized to 900 curves.

After plasma treatment and prior to exposing the sample to toluene vapor, the histogram of the stiffness (a) shows only one sharp peak at 0.997 with a half-width at half-maximum of 0.005. This means that at this stage, i.e., before exposing the polymer to toluene vapor, the covered and uncovered areas have the same stiffness, and we cannot distinguish between them.

Yet we can distinguish covered and uncovered areas by exposing the sample to toluene vapor and letting it swell. After the sample has been in vapor for 2 min. a second series of force−volume measurements was performed. By indenting the sample with a maximum piezo extension of $\delta_{max} = 100$ nm (b), the stiffness shows a broad peak centered at 0.99. The broadening of the peak indicates that covered and uncovered areas have different stiffness, but with such a small indentation it was not possible to distinguish between them.

In two successive measurements at two different locations on the sample we increased the maximum piezo extension, and thereby the maximum load and the indentation depth, to $\delta_{max} = 600$ nm. Now, two well-separated peaks can be recognized in the histograms in Figure 2 (c and d). Hence, applying higher loads, it is possible to distinguish between the stiffness of the covered and of the uncovered areas. In particular, the stiffness of the covered area is smaller than in the measurement with $\delta_{max} = 100$ nm, whereas the peak of the stiffness of the uncovered area does not significantly change. The mean stiffness of the covered polymer is 0.968 (c) and 0.969 (d), with a half width at half-maximum of 0.003 and 0.002, respectively. The mean stiffness of the uncovered polymer is 0.997 and 0.996 with a half-width of 0.004 and 0.003, respectively. These two measurements, performed at two different locations on the surface, permit also to verify the reproducibility of the results obtained and to assess that the elastic properties of the sample are not topography dependent.

After the sample has been exposed to toluene vapor for additional 2 min. (overall exposure of 4 min.), still two peaks can be seen in the histogram (e), and they are even further separated. The lower peak, corresponding to the covered area, has the maximum at 0.942 with a half width at half-maximum of 0.005. The position of the higher peak is unchanged, with the maximum at 1 with a half-width of 0.004.

The stiffness of the uncovered polymer is approximately the same in all measurements (0.996−1), including the one before exposure to toluene vapor. On the other hand, the mean stiffness of the original polymer is lower than after the plasma treatment. This stiffening of the polymer through plasma treatment is a direct proof that the surface is cross-linked.[13]

Also, before exposure to toluene vapor, the stiffness of the covered and uncovered areas are comparable. This points out that a thin cross-linked layer is also formed on the covered regions, even though they are not directly in contact with the plasma. Since measurements of stiffness via indentation are mostly sensitive to the stiffness of the uppermost layer, the two regions cannot be distinguished prior to the exposure to solvent. Upon exposure to the solvent the bulk polymer under the thin surface layer swells and becomes much more compliant, thereby strongly influencing the total measured stiffness. Yet, for small loads, e.g., for $\delta_{max} = 100$ nm, the covered areas have a relatively high stiffness, comparable with that of the uncovered areas, as observed in histogram (b). This is due to the fact that with such small loads, the sample is indented only for some nanometers, and only the uppermost, cross-linked, and therefore, stiff layer is probed. With higher loads, e.g., with $\delta_{max} = 600$ nm, as in the histograms (c) and (d), the sample is indented deeper, also the bulk polymer (swollen and much more compliant) is probed and the measured stiffness decreases considerably. Hence, the differences in the probed stiffness are due to the *depth* of the cross-linked uppermost layer, to the penetration of solvent and to the consequent swelling, and they cannot be determined after the plasma treatment alone without exposure to the solvent.

Let us now relate the mechanical properties of the sample to its topology, by comparing the stiffness maps corresponding to the histograms (c) and (e) and the relative topographies. As shown in Figure 3, two regions can be clearly distinguished in each stiffness map: the bright regions have a mean stiffness between 0.99 and 1 and can be identified, after comparison with the AFM image, with the uncovered areas of the polymer. The gray regions have a lower mean stiffness of about 0.97 (c) or 0.94 (e) and correspond to the covered areas, as can be seen in the graphs on the right side of the stiffness maps, where both topography and stiffness line profiles are reported.

Another phenomenon worth mentioning is that between the swollen area, and the not-swollen one, there is a third area which is more compliant than the other two (represented in dark gray in the maps in Figure 3). This area is narrow in map (c) and becomes wider in map (e), which means that it grows with the swelling time. Moreover, it is on the border between the swollen and the not-swollen areas, so it is reasonable to suppose that the polymer in this region is particularly loose and less compact than in the other two areas. This explains the relatively large distribution of stiffness values in histogram (e). This decrease of the stiffness is superimposed to another effect, present only at the very edge of the swollen areas, since at the edge the contact area decreases out of geometrical reasons, also the stiffness decreases.

The border between the two regions is an edge, where the stiffness

As for the topography, the mechanical properties of the sample, and in particular the stiffness, do not change over time and are stable for weeks.

So far, we discussed the stiffness in the approximation of small deformations. It is affected both by elastic and plastic contributions. However, for a better understanding of the physical processes behind the different outcomes on the different areas of the substrate upon exposure to the solvent, we need to analyze, in detail, the force−distance curves. In Figure 4 are displayed two representative deflection−displacement curves

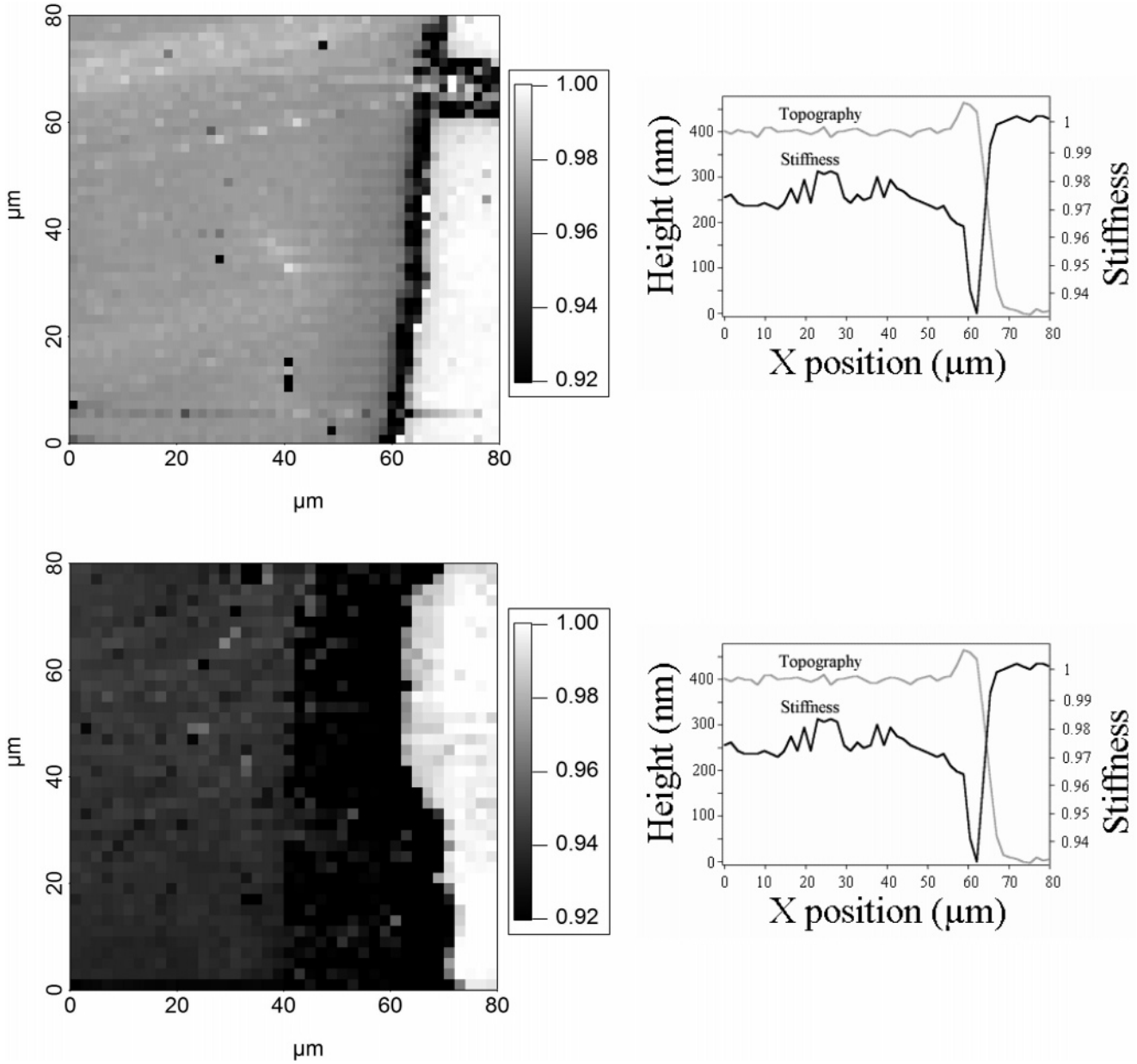

Figure 3. Stiffness maps corresponding to the histograms (c) and (e), respectively top and bottom graphs. At the right sides, two profiles (height and stiffness) are displayed for each map.

acquired on the covered and uncovered polystyrene after 4 min of exposure to toluene vapor. Such curves are typical indentation curves for AFM and differ sensibly from curves acquired with an indentor, mainly due to geometrical and dimensional differences of the tips.[16−20] The curve obtained on the same covered area after 2 min in the toluene vapor lies between the two, but is not shown for clarity. Since the force exerted by the cantilever and its deflection are proportional ($F = k_c\delta$), in the following, we will speak alternately of force and deflection.

We can notice that (1) For deflections below about 200 nm, the two approach contact lines almost overlap; (2) At a certain force the curve on the covered area presents a kink, after which the stiffness decreases; and (3) The retraction contact line of the curve on the covered area does not overlap with the approach contact line like it does for the uncovered area, so that there is a nonzero hysteresis.

The missing hysteresis in the deflection−displacement curves for the uncovered area suggests that even at indentations with $\delta_{max} = 600$ nm the polymer behaves elastically. This is true for the covered area only at the beginning of the curve. The decreasing stiffness after the kink points out that the approach curve, after an initial phase where the tip indents a rather stiff layer of polymer, is influenced by the presence of a more compliant layer underneath. This underlying layer can be plastically deformed, as indicated by the nonzero hysteresis between approach and retraction contact lines and by the presence of permanent deformations (indentation holes) left on the polymer surface after the acquisition of the curves. In the measurement with $\delta_{max} = 100$ nm (Figure 2b) we could not discriminate between the covered and the uncovered areas because the deformation was so small that no plastic deformation was achieved. The measured stiffness was thus not affected by the underlying softer layer, as it was with $\delta_{max} = 600$ nm.

A more quantitative analysis can be performed by calculating the Young's modulus of the polymer. We do this by first calculating the deformation of the polymer through eq 1, and then relating it to the load. The relation between deformation and load is given, depending on the adhesion, by three different contact mechanics theories: the Hertz,[21] the DMT,[22] and the JKR[23] models. Since the tip−sample adhesion is negligible in

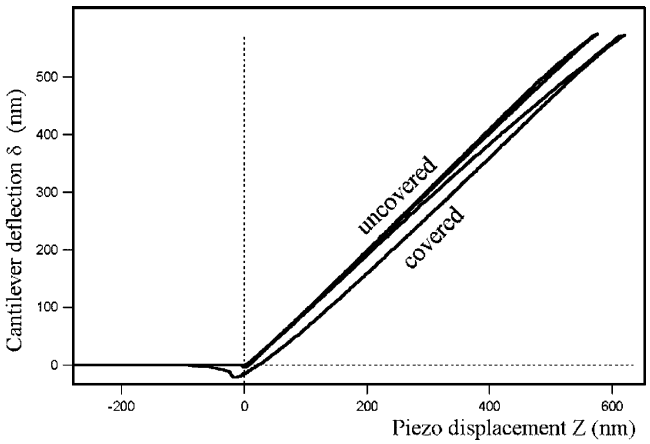

Figure 4. Cantilever deflection−piezo displacement curves within the covered and the uncovered regions of the PS surface after 4 min exposure to toluene vapor.

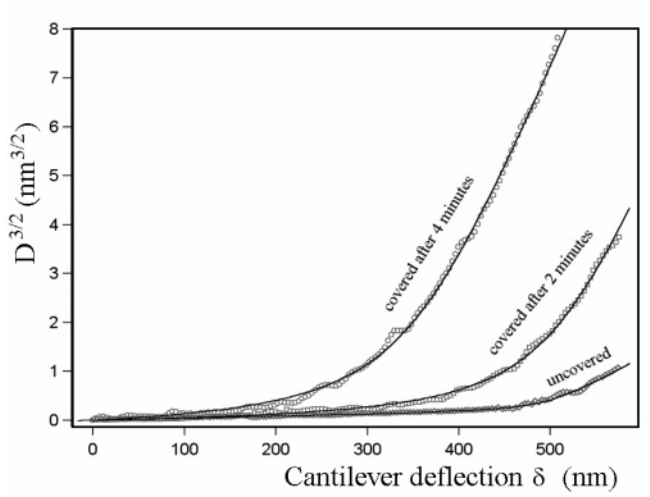

Figure 5. $D^{3/2}$ vs δ plots for the covered and uncovered regions, both after 2 and 4 min exposure to toluene vapor. The experimental data are fitted with eq 5.

comparison to the load, we can apply the Hertz model to the elastic part of the contact line.[15−16] In the Hertz theory, the applied load and the deformation of the sample are related by

$$F = k_c\delta = E_{tot}\sqrt{R}D^{3/2} \Rightarrow D^{3/2} = \frac{3(1-\nu_S^2)}{4}\frac{1}{E}\frac{k_c}{\sqrt{R}}\delta \quad (3)$$

where k_c is the elastic constant of the cantilever, δ the cantilever deflection, R the radius of the tip, and D the sample deformation. It is further assumed that the Young's modulus of the tip E_t is much larger than that of the sample, and hence the total Young's modulus E_{tot} can be approximated by

$$\frac{1}{E_{tot}} = \frac{3}{4}\left(\frac{1-\nu_S^2}{E} + \frac{1-\nu_t^2}{E_t}\right) \cong \frac{3}{4}\frac{1-\nu_S^2}{E} \quad (4)$$

where ν_t and ν_S are the Poisson's ratios of tip and sample, and E is the Young's modulus of the sample. Figure 5 shows the $D^{3/2}$ vs δ plots for the uncovered regions and for the covered ones both after 2 and 4 min of exposure to toluene vapor. As shown in eq 3, when the deformation are purely elastic, a $D^{3/2}$ curve plotted against the deflection should be a line. Instead, the $D^{3/2}$ curves in Figure 5 consist of two linear regions with different slopes. The first region at small deflections is the elastic regime of deformation. The slope of the second region (right side of graph) is larger than that of the first one. In eq 3 the proportionality factor between $D^{3/2}$ and δ, i.e., the slope of the elastic region, is inversely proportional to the Young's modulus of the sample. Hence, a larger slope corresponds to a lower stiffness. This increase of the stiffness is due to (i) the onset of plastic deformations, and (ii) the presence of the more compliant bulk polymer under the cross-linked surface layer. The two linear regions are connected by a third region where the slope is not constant. This region should ideally be a single point, called the *yielding point*, but in polymers there is always a distribution of yielding points, because not all chains yield at the same force and because the stress in the contact area is not uniform.[23]

We then fit the $D^{3/2}$ functions with hyperbolas in the form[17,18]

$$y = D^{3/2}(\delta) = (\beta\delta - \epsilon) + \sqrt{\alpha^2\delta^2 - 2\epsilon(\beta-\gamma)\delta + \epsilon^2} \quad (5)$$

where all parameters are positive and $\beta-\alpha < \gamma < \beta+\alpha$. This fit represents a model which describes the yielding region, and hence the onset of plastic deformation, as a gradual transition from an elastic deformation, where $D^{3/2} \cong \gamma\delta$, to a plastic deformation with lower stiffness, with $D^{3/2} - \gamma\delta_{yield} = (\alpha + \beta)(\delta - \delta_{yield})$. In this model, the plastic deformation thus also shows a linear dependence on the load, but with a different proportionality coefficient and with a different origin of the deformation-deflection plot (δ_{yield} instead of 0). The two deformation regimes are connected by a transition region around the yielding point $\delta_{yield} = \epsilon/\alpha$. Hence, by changing the origin of the $D^{3/2}$ vs δ plot from zero to the yielding point, a plastically deformed polymer can be treated, from the mathematical point of view, as an elastically deformed polymer with smaller stiffness.

From the first part of the $D^{3/2}$ curves it is possible to calculate the Young's modulus of the sample using eq 3. We determined the Young's modulus of the original polystyrene substrate with this model. We obtained a value of about 3 GPa, in accordance with a stress−strain measurement ($E = 3.18$ GPa), and with the value provided by the manufacturer ($2.3 < E < 4.1$ GPa) and data from literature.[18,24] The determination of the Young's modulus of the original polystyrene permits also to give an estimation of the tip radius R. The tip radius has been chosen to $R = 20 \pm 5$ nm, to match the Young's modulus of the untreated polymer given by the manufacturers. By checking the shape of the indented holes before and after the experiments we could see that the tip did not wear during the experiments, as plausible for such small loads.

Turning to the Young's modulus of the plasma and solvent exposed polystyrene, both in the covered and in the uncovered areas, we measured a much higher value than on the original polystyrene. A more precise value for the Young's modulus cannot be calculated, since the cross-linked sample has become very stiff through cross-linking generated by the plasma treatment, and the cantilever elastic constant is now lower than that of the sample, so that the small deformations are at the limit of resolution of the AFM and we probe primarily the mechanical properties of the cantilever (see eq 2).

The value of the Young's modulus in the initial, elastic part of the contact line is highest on the uncovered area, becomes slightly smaller on the covered area after 2 min swelling, and is even smaller after 4 min swelling. The analogue of the Young's modulus measured after the onset of the small plastic deformations (inversely proportional to the parameter $\alpha + \beta$ in eq 5) is about 3 GPa. This value is a composition of the very high Young's modulus of the superficial layer and of that of

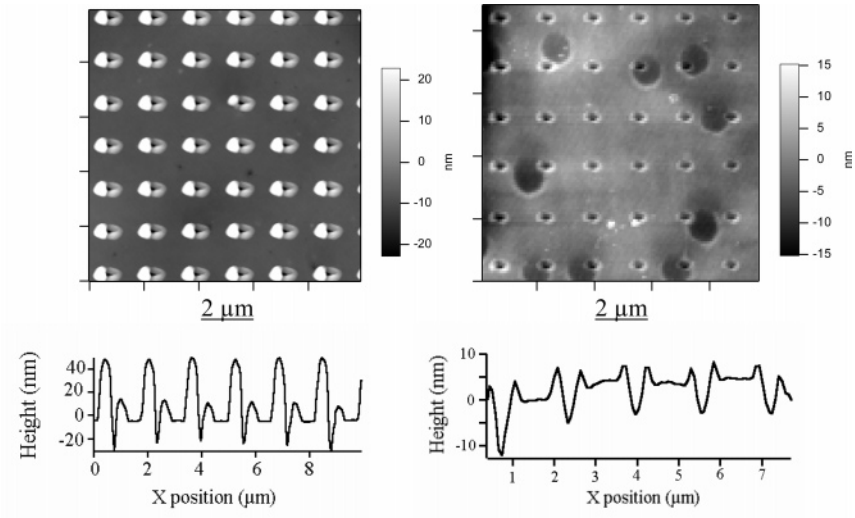

Figure 6. Topography of the swollen and of the uncovered surface after force−distance curves acquisition in force−volume mode, showing the holes resulting from the indentation of the tip during the acquisition of the force−displacement curves. Also the corresponding profiles of the holes are shown.

the bulk polymer after solvent exposure, and shows that the Young's modulus of the bulk polystyrene under the cross-linked layer is smaller than that of the original polymer. Considering these results we can draw the following picture of the phenomena involved in plasma treatment and successive swelling:

(1) The plasma generates a stiff polymer layer, both on the area shadowed by the mask and on the exposed area. This stiffer surface layer is formed by cross-linked polymer. The mask influences only the thickness and the cross-linking of the uppermost layer.

(2) The solvent penetrates and diffuses into the polymer, softens it, and makes it likely to be plastically deformed. The two areas, covered and uncovered, exhibit different swelling behavior; the protrusions of the first are higher than the protrusions of the second, because the deeper cross-linked superficial layer on the uncovered regions hinders polymer chains from expanding.

(3) After swelling, the stiffness of the underlying softer bulk polymer also affects the probed stiffness of the upper layer. The probed stiffness depends on the amount of solvent absorbed, and on the thickness of the cross-linked layer.

(4) The onset force for plastic deformations (yielding force) depends on the amount of solvent absorbed.

Hence, the uncovered surface can be plastically deformed only at relatively high forces, and the stiffness of the cross-linked surface layer is practically not affected by the underlying compliant bulk polymer.

The yielding force on the regions covered by the mask is considerably lower, and the compliant layer affects the stiffness of the cross-linked one since the very beginning of the curve.

The previous considerations are confirmed by the calculation of the energy dissipated in the sample due to the plastic deformation, defined as the area between the approach and the retraction force−distance curves above the zero axis. In measurement (b), with $\delta_{max} = 100$ nm, the dissipated energy is similar on the covered and on the uncovered areas (60 ± 20 fJ). This confirms that no plastic deformations take place, and that for small forces, the deformation is purely elastic. The value of the dissipated energy on the uncovered areas is the same for all other measurements (c−e). In contrast, the dissipated energy is much larger on the covered, swollen polymer in measurement (c) (300 ± 15 fJ), and (e) (500 ± 80 fJ), indicating that plastic deformations take place.

Further confirmations and insights can be obtained by looking at the surface of the polymer after the deformations caused by the force−volume measurements. Figure 6 shows the topographies of the swollen and of the uncovered surface after measurement. On the uncovered surface the holes carved by indentation are 7 ± 2 nm deep with some piled-up polymer around, whose volume is comparable to that of the holes. The holes on the covered surface are 20 ± 3 nm deep, and they are surrounded by a rather large amount of piled-up material, whose volume is larger than that of the holes. This confirms that the plastic deformations on the uncovered areas are very small. The asymmetric profile of these deeper holes (a common phenomenon in AFM indentation) is due to the tilt angle of the cantilever.

Usually a parameter called "plasticity index", ψ, is used to describe the relative plastic/elastic character of the sample.[25] It is defined from the topography of the deformation as $\psi = A_p/A_n$, where A_p is the cross-sectional area of the piled-up material and A_n is the cross-sectional area of the carved hole. For ideal microcutting (no piled-up material) $\psi = 0$, and for ideal microploughing (the cross-sectional area of the piled-up material is the same as that of the hole) $\psi = 1$. In our experiment, the indentation on the plasma-exposed material is either purely elastic or, for larger forces, close to microcutting. This indicates that most of the material in the indented area is compressed, and only a very small portion of the polymer is piled up. On the swollen polymer, we find $\psi > 1$. A plasticity index larger than 1 is not allowed by definition but was observed in several experiments.[26−29] This is due to the fact that the plastic deformation, leading to a compression of the material in the indented area, is accompanied by large displacements of the soft polymer. Such a volume increase implies a decrease in the density of the polymer, i.e., the pile-ups do not consist of compacted, packed material, but are instead loose material aggregates that were pushed out sidewise during the indentation.[27,29] The large pile-ups in the covered areas show that the polymer chains in these regions have a higher mobility, due to the solvent, and is a confirmation of the stiffness and elastic-plastic properties measurements.

Conclusions

In the present work, we have studied the effect of a local air plasma treatment of polystyrene on the mechanical properties of the polymer by indentation in the elastic and plastic regime. The local exposure to plasma was achieved by means of a mask, covering some regions of the sample and providing uncovered and covered areas.

A first measurement on the treated sample could not show any differences in the elastic−plastic properties of the polymer in the two regions. Instead, an increased stiffness with respect to that of the unmodified sample has been measured in both regions. This result, corroborated by other measurements, leads to the hypothesis that an uppermost layer of the polymer is cross-linked due to plasma radiation. The plasma radiation penetrates also the regions covered by the mask.

To emphasize the differences of the covered and uncovered areas, the sample has been exposed to solvent vapor for different times. The solvent, penetrating the uppermost cross-linked layer, let the bulk polymer soften. In the covered areas, where the cross-linked layer is less deep than on the uncovered areas, the polymer can swell and protrude.

After exposure to solvent, the stiffness of the underlying softer bulk polymer affects the measured stiffness. Hence, the probed stiffness of the covered areas decreases considerably and depends on the exposure time, whereas the measured stiffness on the uncovered areas does not change but very little.

Also plastic deformations are influenced by adsorption of solvent and swelling, and they occur on the covered areas at lower forces, as shown by the analysis of the force−displacement curves. As evidenced by the measurement of the energy dissipated in the sample and by the topography of the sample after force−volume acquisition, plastic deformations, i.e., the holes carved by the force−displacement curves, are larger on the covered areas than on the uncovered ones.

Our results suggest that indentation is a valuable tool to resolve the coupling mechanism between local variations in the mechanical properties of polymer surfaces and surface structuring. Additionally we present, to our knowledge, the first direct evidence that plasma causes cross-linking of polymer surfaces.

References and Notes

(1) Folch, A.; Toner, M. *Annu. Rev. Biomed. Eng.* **2000**, *2*, 227.

(2) Squires, T. M.; Quake, S. R. *Rev. Mod. Phys.* **2005**, *77*, 977.

(3) Delamarche, E.; Juncker, D.; Schmid, H. *Adv. Mater.* **2005**, *17*, 2911.

(4) Blackman, G. S.; Lin, L.; Matheson, R. R. *Polym. Preprints* **1998**, *39*, 1218.

(5) Zhao, X. M.; Xia, Y.; Schueller, O. J. A.; Qin, D.; Whitesides, G. M. *Sens Actuators A* **1998**, *65*, 209.

(6) Bowden, N.; Brittain, S.; Evans, A. G.; Hutchinson, J. W.; Whitesides, G. M. *Nature* **1998**, *393*, 146.

(7) Stafford, C. M.; Harrison, C.; Beers, K. L.; Kaarim, A.; Amis, E. J.; VanLandingham, M. R.; Kim, H.-C.; Volksen, W.; Miller, R. D.; Simonyi, E. E. *Nat. Mater.* **2004**, *3*, 545.

(8) Katzenberg, F. *Macromol. Mater. Eng.* **2001**, *286*, 26.

(9) Bonaccurso, E.; Graf, K. *Langmuir* **2005,** *20*, 11183.

(10) Elbs, H.; Fukunaga, K.; Stadler, R.; Sauer, G.; Magerle, R.; Krausch, G.; *Macromolecules* **1999**, *32*, 1204.

(11) Bonaccurso, E.; Butt, H.-J.; Graf, K. *Eur. Polym. J.* **2004**, *40*, 975.

(12) Knittel, D.; Kesting, W.; Schollmeyer, E. *Polym. Int.* **1997**, *43*, 231.

(13) Larsson, A.; Dérandy, H. *J. Colloid Interface Sci.* **2002**, *246*, 214.

(14) Büscher, K.; Berger, R.; Brünger, W.; Graf, K. accepted by *Microelectron. Eng.* **2006**.

(15) Cappella, B.; Dietler, G. *Surf. Sci. Rep.* **1999**, *34*, 1.

(16) Butt, H.-J.; Cappella, B., Kappl, M. *Surf. Sci. Rep.* **2005**, *59*, 1.

(17) Cappella, B.; Kaliappan, S. K. *Macromolecules* **2005**, *38*, 1874.

(18) Kaliappan, S. K.; Cappella, B. *Polymer* **2005**, *46*, 11416.

(19) Reynaud, C.; Sommer, F.; Quet, C.; El Bounia, N.; Duc, T. M. *Surf. Interface Anal.* **2000**, *30*, 185.

(20) Du, B.; Liu, J.; Zhang, Q.; He, T. *Polymer* **2001**, *42*, 5901.

(21) Hertz, H. *J. Reine Angew. Math.* **1881**, *92*, 156.

(22) Derjaguin, B. V.; Müller, V. M.; Toporov, Yu. P. *J. Colloid Interface Sci.*, **1975**, *53*, 314.

(23) Johnson, K. L.; Kendall, K.; Roberts, A. D. *Proc. R. Soc. London A* **1971**, *324*, 301.

(24) Lubarsky, G. V.; Davidson, M. R.; Bradley, R. H. *Surf. Sci.* **2004**, *558*, 135.

(25) Han, Y.; Schmitt, S.; Friedrich, K. *Appl. Comput. Mater.* **1999**, *6*, 1.

(26) Khurshudov, A.; Kato, K.; *J. Vac. Sci. Technol. B* **1995**, *13*, 1938.

(27) Hamada, E.; Kaneko, R.; *Ultramicroscopy* **1992**, *42*−*44*, 184.

(28) Aoike, T.; Yamamoto, T.; Uehara, H.; Yamanobe, T.; Komoto, T. *Langmuir* **2001**, *17*, 5688.

(29) Cappella, B.; Sturm, H. *J. Appl. Phys.* **2002**, *91*, 506.